Drug and Chemical Toxicology

ISSN: 0148-0545 (Print) 1525-6014 (Online) Journal homepage: https://www.tandfonline.com/loi/idct20

Design and synthesis of novel organometallic complexes using boronated phenylalanine derivatives as potential anticancer agents

Mehmet Varol, Kadriye Benkli, Ayşe T. Koparal & Rakibe B. Bostancıoğlu

To cite this article: Mehmet Varol, Kadriye Benkli, Ayşe T. Koparal & Rakibe B. Bostancıoğlu (2019) Design and synthesis of novel organometallic complexes using boronated phenylalanine derivatives as potential anticancer agents, Drug and Chemical Toxicology, 42:4, 436-443, DOI: 10.1080/01480545.2018.1504057

To link to this article: https://doi.org/10.1080/01480545.2018.1504057

DRUG AND CHEMICAL TOXICOLOGY
2019, VOL. 42, NO. 4, 436–443
https://doi.org/10.1080/01480545.2018.1504057

Taylor & Francis
Taylor & Francis Group

RESEARCH ARTICLE

Design and synthesis of novel organometallic complexes using boronated phenylalanine derivatives as potential anticancer agents

Mehmet Varol[a,b], Kadriye Benkli[c,d], Ayşe T. Koparal[b] and Rakibe B. Bostancıoğlu[b]

[a]Department of Molecular Biology and Genetics, Mugla Sitki Kocman University, Mugla, Turkey; [b]Faculty of Science, Department of Biology, Anadolu University, Eskisehir, Turkey; [c]Department of Pharmaceutical Chemistry, Faculty of Pharmacy, Bezmialem Vakif University, İstanbul, Turkey; [d]Faculty of Pharmacy, Department of Pharmaceutical Chemistry, Anadolu University, Eskisehir, Turkey

ABSTRACT

Drug design and discovery studies are important because of the prevalence of diseases without available medical cures. New anticancer agents are particularly urgent because of the high mortality rate associated with cancer. A series of mononuclear gold (III) and platinum (II) complexes based on boronated phenylalanine (BPA) were designed and synthesized using 4,4′-dimethyl-2,2′-dipyridyl (L1) or 1,10-phenanthroline-5,6-dion (L2) ligands to obtain promising anticancer drug candidates. Proton nuclear magnetic resonance, infrared, mass spectrometry, and elemental analyses were utilized for chemical characterizations. Cell viability, cancer cell colony formation, endothelial tube formation, and cytoskeleton staining assays were performed using A549 lung adenocarcinoma and human umbilical vein endothelial cells (HUVECs) to investigate preliminary pharmacological activities. L1-based platinum (II) complex (BPA-L1-Pt) was the most promising complex, and has similar activity with the approved chemotherapy drug cis-platinum. Half maximal inhibitory concentration values for BPA-L1-Pt were 9.15 μM on A549s and 16.61 μM on HUVECs; the values for cis-platinum were 5.24 μM on A549s and 23.14 μM on HUVECs. Consequently, further synthesis studies should be performed to boost the cancer cell selectivity feature of BPA by varying metal and ligand types.

ARTICLE HISTORY
Received 26 February 2018
Revised 29 June 2018
Accepted 19 July 2018

KEYWORDS
Angiogenesis; drug design; cell survival; cisplatin (CAS Number: 15663-27-1); 4-dihydroxyborylphenylalanine (CAS Number: 76410-58-7)

Introduction

Clinical utilization of cisplatin has heralded the age of metal-based anticancer therapeutics allowing for new platinum-based drugs such as carboplatin, oxaliplatin, nedaplatin, lobaplatin, and satraplatin (Alderden *et al*. 2006, Wheate *et al*. 2010, Ali *et al*. 2013, Liu and Gust 2013). Gold-based complexes are also under investigation because of the isoelectronic features of gold (III) and Pt (II) metals with each other (Ronconi *et al*. 2006, Frezza *et al*. 2011). Moreover, cisplatin has the same square-planar geometry with tetra-coordinate gold (III) complexes, which are promising anticancer therapeutics (Chen *et al*. 2009, Nobili *et al*. 2010). Numerous studies elucidate the anticancer activity of platinum and gold complexes (Bostancioglu *et al*. 2012, Serratrice *et al*. 2012, Sun 2013). On the other hand, the possible side effects (such as vomiting, myelosuppression, nephropathy and nephrotoxicity, and gastrointestinal and hematological toxicity) and drug resistance phenomena of the approved platinum complexes have compelled pharmacologists to design and discover new metal-based therapeutics (Serratrice *et al*. 2012, Sun 2013, Liu and Gust 2013, Corte-Real *et al*. 2014, Varol 2016). Employing already known active compounds is a rational way to design new anticancer drugs to overcome their disadvantages and increase their functionality. One of these functional molecules is 4-dihydroxyborylphenylalanine (*BPA*, CAS Number: 76410-58-7), a boron delivery agent (Miyatake *et al*. 2016). *BPA* is a boronated amino acid (phenylalanine) used in boron neutron capture therapy (BNCT), which is an experimental and noninvasive cancer treatment (Aihara *et al*. 2006, Henriksson *et al*. 2008). *BPA* is a promising compound because of its ability to transport across the cell membrane through the L-amino-acid-transport system (Heber *et al*. 2006, Yokoyama *et al*. 2006). Additionally, the cellular uptake of *BPA* depends on metabolic rate, and that dependency can be exploited for the selective uptake of *BPA*-based anticancer agents by capitalizing on the relatively high metabolism and proliferation rate of cancer cells in the body (Zhao *et al*. 2013, Keibler *et al*. 2016). Therefore, we designed and synthesized new organometallic complexes based on boronated phenylalanine (*BPA*) for the first time. Their pharmacological activities were preliminary investigated using A549 lung adenocarcinoma cells and human umbilical vein endothelial cells (HUVECs) using cell viability, cancer cell colony formation, endothelial tube formation, and cytoskeleton alteration assays.

Materials and methods

Materials

Roswell Park Memorial Institute-1640 (RPMI-1640) medium was obtained from Gibco (Grand Island, NY, USA). Nutrient

CONTACT Mehmet Varol mehmetvarol@mu.edu.tr, mehmetv@hotmail.it Faculty of Science, Department of Molecular Biology and Genetics, Mugla Sitki Kocman University, Kotekli Campus, Mugla TR48000, Turkey

mixture Ham's F-12 K medium (F-12 K), thiazolyl blue tetrazolium bromide (MTT), TRITC-phalloidin, Matrigel, agar powder, and other reagents were obtained from Sigma-Aldrich (St Louis, MO, USA). Round glass coverslips and tissue culture plates were purchased from Marienfeld (Lauda-Königshofen, Germany) and TPP (Trasadingen, Switzerland), respectively.

Chemical synthesis and characterization

Organometallic complexes were prepared by the reaction of equimolar (0.1 M) BPA, 4,4′-dimethyl-2,2′-dipyridyl (*L1*; CAS Number: 1134-35-6) or 1,10-phenanthroline-5,6-dion (*L2*; CAS Number: 27318-90-7), and potassium tetrachloroplatinate(II) (CAS Number: 10025-99-7) or sodium tetrachloroaurate(III) dehydrate (CAS Number: 13874-02-7) in methanol for 2 h at 60 °C. The mixture was kept at room temperature for 8–10 h. After cooling, the precipitate was collected and washed with diethyl ether. The filtered precipitate was dried using a vacuum desiccator. All reactions were performed in the dark and controlled using thin layer chromatography (silica gel 60G F_{254}) with the solvent system petroleum ether:ethyl acetate:ethanol (2:2:1). The synthesis procedures are shown in Figure 1(A). Geometric and electronic structures of the synthesized complexes were optimized using Gaussian 03 software with HF theory at the B3LYP/3-21G level (Figure 1(B)). Proton nuclear magnetic resonance (^{1}H-NMR) spectra were run on a Bruker 400 MHz using tetramethylsilane internal standard and DMSO-d_6 solvent. Schimadzu 8400 FTIR, VG Quattro, Perkin Elmer EAL 240, and Electrothermal IA9100 digital melting point apparatuses were used to obtain infrared (IR), mass spectrometry (MS), elemental, and melting point data, respectively. All spectral analyses were performed at AUBIBAM, Anadolu University.

(4-(2-Amino-2-(2,10-dimethyl-6H-imidazo[1,5-a;3,4-a′] dipyridin-6-yl)ethyl)phenyl) boronic acid Au(III) complex (BPA-L1-Au): Reaction efficiency: 60%. Purity: 99.84%. Melting point: >300 °C. Rf value: 0.6. IR (KBr) ν_{max} (cm^{-1}): 3441, 3345; 3065; 2924; 2855; 1615, 1568, 1464; 1335, 1267, 1175, 1029; 817, 742; 696; 653. ^{1}H-NMR (400 MHz) (DMSO-d_6) δ (ppm): 4.6–4.8 (2H, m), 5.0–5.2 (1H, m), 6.2–6.3 (1H, m), 8.7–10.0 (17H, m), 10.1–10.2 (1H, bs), 10.4–10.6 (2H, bs). Anal calcd for $C_{21}H_{24}BN_3O_2Cl_2Au$: C, 40.09%; H, 3.85%; N, 6.68%, found: C, 40.42%; H, 3.52%; N, 6.54%. MS (EI): *m/z* calcd 628.10, found 627.09 (M+).

*(4-(2-amino-2-(10,11-dioxo-10,11-dihydro-5H-imidazo[1,5,4,3-lmn][1,10]phenanthroline-5-yl)ethyl)phenyl) boronic acid Au(III) complex (BPA-L2-Au)***:** Reaction efficiency: 45%. Purity: 99.85%. Melting point: >300 °C. Rf value: 0.5. IR (KBr) ν_{max} (cm^{-1}): 3389, 3358; 3079; 2943; 2868; 1573, 1489, 1460; 1329, 1277, 1146, 1020; 812, 745; 710; 644. ^{1}H-NMR (400 MHz) (DMSO-d_6) δ (ppm): 3.00–3.20 (2H, d), 4.3–4.4 (1H, t), 6.6–6.8 (4H, dd), 7.0–7.8 (8H, m), 7.8–8.0 (1H, bs), 8.5–8.8 (2H, bs). Anal calcd for $C_{21}H_{18}BN_3O_4Cl_2Au$: C, 38.50%; H, 2.77%; N, 6.41%, found: C, 38.72%; H, 2.42%; N, 6.74%. MS (EI): *m/z* calcd 654.04, found 653.04 (M+).

*(4-(2-Amino-2-(2,10-dimethyl-6H-imidazo[1,5-a;3,4-a′]dipyridin-6-yl)ethyl)phenyl) boronic acid Pt(II) complex (BPA-L1-Pt)***:** Reaction efficiency: 63%. Purity: 99.84%. Melting point: 292–297 °C. Rf value: 0.8. IR (KBr) ν_{max} (cm^{-1}): 3426, 3348; 3067; 2928; 2841; 1619, 1564, 1466; 1336, 1283, 1195, 1029; 818, 749; 712; 678. ^{1}H-NMR (400 MHz) (DMSO-d_6) δ (ppm): 4.6–4.9 (4H, m), 5.9–8.2 (17H, m), 8.4–8.5 (1H, bs), 8.9–9.0 (2H, bs). Anal calcd for $C_{21}H_{24}BN_3O_2Cl_2Pt$: C, 40.21%; H, 3.86%; N, 6.70%, found: C, 40.41%; H, 3.97%; N, 6.54%. MS (EI): *m/z* calcd 626.10, found 625.09 (M+).

*(4-(2-amino-2-(10,11-dioxo-10,11-dihydro-5H-imidazo[1,5,4,3-lmn][1,10]phenanthroline-5-yl)ethyl)phenyl) boronic acid Pt(II) complex (BPA-L2-Pt)***:** Reaction efficiency: 60%. Purity: 99.85%. Melting point: >300 °C. Rf value: 0.8. IR (KBr) ν_{max} (cm^{-1}): 3449, 3368; 3066; 2942; 2854; 1643, 1555, 1451; 1338, 1265, 1177, 1028; 820, 745; 700; 666. ^{1}H-NMR (400 MHz) (DMSO-d_6) δ (ppm): 3.2–3.3 (2H, d), 4.3–4.4 (1H, bs), 6.6–6.7 (4H, dd), 6.8-8.4 (8H, m), 8.5–8.6 (1H, bs), 8.9–9.1 (2H, bs). Anal calcd for $C_{21}H_{18}BN_3O_4Cl_2Pt$: C, 38.62%; H, 2.78%; N, 6.43%, found: C, 38.98%; H, 3.02%; N, 6.56%. MS (EI): *m/z* calcd 652.04, found 651.03 (M+).

Cell culture

Human lung adenocarcinoma (A549) cells and HUVECs were purchased from Institute for Fermentation (IFO, Osaka, Japan)

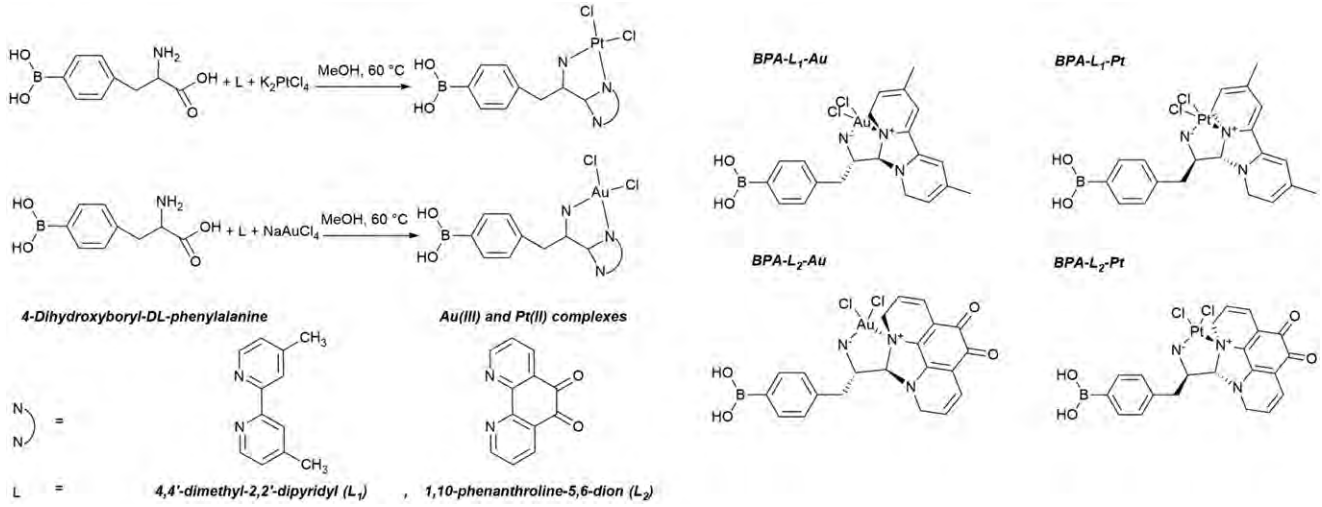

Figure 1. Synthesis procedures of the organometallic complexes (A) and chemical structures of the synthesized *BPA*-based complexes (B).

and American Type Culture Collection (ATCC), respectively. A549 cells were maintained in a monolayer in RPMI-1640 containing 10% FBS, 1% penicillin-streptomycin, and sodium bicarbonate. HUVECs were maintained in a monolayer in nutrient mixture Ham's F-12K containing endothelial cell growth supplement, 20% FBS, 1% penicillin-streptomycin, and sodium bicarbonate. A549s and HUVECs were incubated at 37 °C in a 5% CO_2 humidified incubator. Stock solutions of the complexes were initially prepared in DMSO and diluted in fresh medium.

Proliferation assay

Antiproliferative influences of the complexes were identified through mitochondrial metabolic activity using the MTT cell viability assay as previously described (Mosmann 1983, Rosselli *et al*. 2012). A549s and HUVECs were treated with 12.5, 25, 50, 100, 200, and 400 μM concentrations of the complexes for 24, 48, and 72 h; eight replicate wells were used for each concentration and the assays were repeated in triplicate at different times. The approved anticancer drug, Cis-diammineplatinum (II) dichloride (CAS Number: 15663-27-1) was the positive control. Absorbance was measured at 570 nm using a Bio-Tek ELX808IU microplate reader.

Cancer cell colony formation assay

The double layer soft agar (3% select-agar over a base of 6% select-agar) method in 6-well microplates was performed to determine the anchorage-independent growth potential of A549s (1×10^3 cells/well) treated with 25, 50, 100, and 200 μM of the complexes, as previously described (Bostancioglu *et al*. 2012). Three replicate wells per concentration were used and repeated in triplicate at different times. Cells were incubated for 15 days at 37 °C in a 5% CO_2 humidified incubator. Colony formation was observed every 5 days. After 15 days, the colonies with more than 50 cells were counted.

Cytoskeleton integrity

Stress actin proteins were stained using the method previously described (Rubin *et al*. 1991, Varol *et al*. 2016). A549s (12×10^3 cells/well) on glass coverslips in a 6-well plate were incubated for 24 h and treated with different concentrations of the complexes for 24 h. After the treatment period, the cells were fixed, permeabilized, washed, and stained with 3.7% paraformaldehyde (15 min), 0.5% Triton X-100 (5 min), PBS (three times), and 5 μg/ml tetramethylrhodamine B isothiocyanate (TRITC)-labeled phalloidin (1 h) at 37 °C, respectively. Actin filaments were photographed using an Olympus BX50 microscope with the U-UHK fluorescence attachment and DP70 camera at 100× magnification.

Matrigel tube formation assay

The endothelial tube formation assay is an established method for *in vitro* modeling of angiogenesis in drug discovery and design studies. Serum starved endothelial cells arrange themselves into a capillary-like network structure within 12 h of plating on Matrigel (Çağır *et al*. 2017). This assay was performed as previously described (Ouchi *et al*. 2004). Briefly, HUVECs were maintained in endothelial cell basal medium-2 (EBM-2) with 2% FBS for serum starvation. After 6 h serum starvation, the cells were plated in 96-well cell culture plates at a seeding density of 4×10^4 cells/well in the Matrigel-coated wells, which were equilibrated with EBM-2 medium containing the concentrations of the complexes. The endothelial cells were observed and photographed using an Olympus IX70 inverted microscope at 10× magnification.

Statistical analysis

Obtained data from MTT and colony formation assays were evaluated using one-way analysis of variance followed by Tukey's test in statistical package for social sciences software. The experimental study results given in the figures were expressed according to the percentages of control as the mean ± standard deviation. Asterisks indicate significant difference from the control group by the Tukey test ($p < 0.05$). Half maximal inhibitory concentration (IC_{50}) values of the complexes were calculated using nonlinear regression analysis in GraphPad Prism 6 software. Additionally, the figures and photographs were organized in TIFF format using Adobe Photoshop CS6 after the figures were created in MS Office.

Results

Chemistry

Infrared spectral analysis indicated that the observed spectra were similar to each other, most likely because of the structural resemblances of the complexes. Nine different band spectra were observed for each complex: amine N-H stretch bands (3345–3449 cm^{-1}), aromatic C-H stretches (3065–3079 cm^{-1}), aliphatic C-H asymmetrical stretches (2924–2943 cm^{-1}), aliphatic C-H symmetrical stretches (2841–2868 cm^{-1}), C = N and C = C stretches (1451–1643 cm^{-1}), C-N stretches (1020–1338 cm^{-1}), out of plane C-H bending bands (742–820 cm^{-1}), metal-N stretches (696–7120 cm^{-1}), and metal-Cl stretch bands (644–678 cm^{-1}). In the ^{1}H-NMR spectra, all protons were at high ppm values because of the influence of the metals. The protons in the platinum complexes had higher ppm values than in the gold complexes. The chemical shifts of N-H protons in the complexes were not clearly observed because the N-H protons in heterocyclic rings in the bridge ligands are very active and can move easily between nitrogen elements. On the other hand, spectra showed the densities and separations in aromatic regions due to steric, conjugative, and inductive effects. The obtained data from elemental analyses and MS were as expected.

Pharmacology

Cytotoxic activities of the organometallic complexes were observed using the MTT assay in order to assess the effects

Table 1. IC_{50} values (μM) of the complexes after exposure for two days.

Complex	A549	HUVEC
BPA-L1-Au	97.98 ± 2.75	123.17 ± 1.6
BPA-L1-Pt	9.15 ± 0.20	16.61 ± 0.39
BPA-L2-Au	17.86 ± 0.49	7.82 ± 0.18
BPA-L2-Pt	14.04 ± 0.31	9.74 ± 0.22
Cis-diammineplatinum (II) dichloride	5.24 ± 0.12	23.14 ± 0.62

on mitochondrial metabolic activities in cancerous A549s and noncancerous HUVECs. IC_{50} values of the complexes and cis-diammineplatinum (II) dichloride after two days exposure are in Table 1. Most of synthesized complexes showed concentration- and time-dependent activities in both cell lines (Figure 2). *BPA-L1-Pt* and *BPA-L1-Au* showed similar activity to cis-diammineplatinum (II) dichloride that was more cytotoxic for A549 adenocarcinoma cells than HUVECs (Figure 2). However, *BPA-L2-Pt* and *BPA-L2-Au* were more active on HUVECs than A549 cells (Figure 2 and Table 1) demonstrating a lack of selectivity for cancer cells. Therefore, the boosting or reducing of the selective feature of *BPA* depends on the types of ligands, as can be seen with the *L1* or *L2* containing complexes. *BPA-L1-Pt* was the most cytotoxic complex on cancer cells with approximately ten times more activity than *BPA-L1-Au*.

Soft agar colony forming assays were performed to assess the effects of the synthesized complexes on A549 cell division capacity using 25, 50, 100, and 200 μM of the complexes. The data verified that the synthesized complexes have time-dependent functionality, and they can inhibit the anchorage-independent growth property of A549 cells, except for 25 μM *BPA*-based Au (III) complexes (Figure 3).

Cancerous cell lines show high migration capacity to escape their stressful microenvironment using migration components such as the actin cytoskeleton. Morphologies of filamentous actin proteins under the influence of the synthesized complexes were examined using TRITC-phalloidin (Figure 4). A549 cells generally displayed a well-organized cytoskeleton morphology. However, the synthesized organometallic complexes caused actin protein aggregations, less actin clusters, and a fuzzy network of shorter actin filaments in a concentration-dependent manner. *BPA-L1-Au* showed low cytoskeletal activity, whereas *BPA-L2-Au* was the most active complex for the disruption of cytoskeleton integrity.

Moreover, to explore the activity of the synthesized organometallic complexes on angiogenesis, we used cultured endothelial cells on Matrigel to assess the creation of tube-like network structures resembling capillary blood vessels characteristic of angiogenesis. A capillary-like tube network of HUVECs was precisely formed in untreated and solvent treated groups (Figure 5). The *BPA-L1-Au* complex dose-dependently decreased endothelial tube formation beginning at 50 μM, and HUVECs were clearly disorganized at the 100 and 200 μM doses. On the other hand, a different effect was observed on the formation of the endothelial network structure for *BPA-L1-Pt*. The applied concentrations of *BPA-L1-Pt* caused organized but disconnected structures for tube-like networking in HUVECs. Moreover, *BPA-L2-Au* and *BPA-L2-Pt* displayed similar antiangiogenic influences for the applied concentrations (Figure 5).

Discussion

DNA is the major target of antitumor compounds and metal complexes are DNA binding agents (Gao *et al*. 2011, Corte-Real *et al*. 2014). Current data in biomedical studies show several other targets for cisplatin inhibition of metabolism in cancer cells, such as targeting glycolytic enzymes and glycolysis regulators (Corte-Real *et al*. 2014). Moreover, the functionalities of gold complexes might be due to their activities on mitochondria, chromosomes, specific kinases, and proteasomes (Sun 2013, Liu and Gust 2013). Thus, anticancer activities of the synthesized complexes were identified using the MTT cell viability assay, and the *L1* complexes generally showed a selective cytotoxic activity on the A549 lung adenocarcinoma cells. On the other hand, numerous studies indicate that cancer cell growth in soft agar is an excellent model for tumorigenicity studies and is closely associated with the transformed property of cancer cells (Bost *et al*. 1999, Kreja and Seidel 2002). In correlation with cell viability assays, the complexes showed an inhibitory activity on the anchorage-independent growth of human lung adenocarcinoma cells. Abnormal cell migration drives the progression of many diseases, including the spread of cancer (Yamaguchi *et al*. 2005, Dart 2016). Metastasis is a multi-stage and complex cellular process, which requires motility of the wandering cancer cell (Sahai 2005). Migration of eukaryotic cells could be driven by polymerization of actin monomers into actin filaments. Thus, cell motility control via actin cytoskeleton formation could provide a mechanism to regulate cancer cell invasion and metastasis (Yamaguchi *et al*. 2005, Condeelis *et al*. 2005, Sahai 2005). Here, *BPA-L2-Au* was the most destructive compound on filamentous actin structures.

Angiogenesis is a hallmark of most neoplastic and non-neoplastic degenerative diseases such as cancer, chronic inflammation, diabetes, and many more, and it is pivotal for the spread of these diseases (Carmeliet and Jain 2000). The formation of new capillary vessels is necessary for tumor tissue formation and growth because cancer cells are desperate, in the absence of veining, to obtain nutrients and oxygen as well as to evacuate metabolic waste and carbon dioxide (Carmeliet and Jain 2000, Hanahan and Weinberg 2011). Therefore, the antiangiogenic activities of the synthesized complexes were investigated using endothelial tube formation assays and *BPA-L2-Au* and *BPA-L2-Pt* showed significant and promising antiangiogenic activity. Thus, the significant antiangiogenic activity of *BPA-L2-Au* was in concert with its activity on filamentous actin proteins.

Many biological processes and homeostasis mechanisms require metal ions as essential components (Aisen *et al*. 2001, Andreini *et al*. 2008, Mjos and Orvig 2014). Thus, cells have sophisticated and sensitive systems for metal ion transport and distribution (Mjos and Orvig 2014). Metal-based complexes are important in medicinal chemistry to design and synthesize novel drugs because of these transport mechanisms (Komeda and Casini 2012, Wang *et al*. 2015). In addition to the cellular transport mechanisms for metals, the possible transport of *BPA* across the cell membrane using the L-amino-acid transport system, which depends on cellular metabolism, was employed in this study. Cellular uptake rates

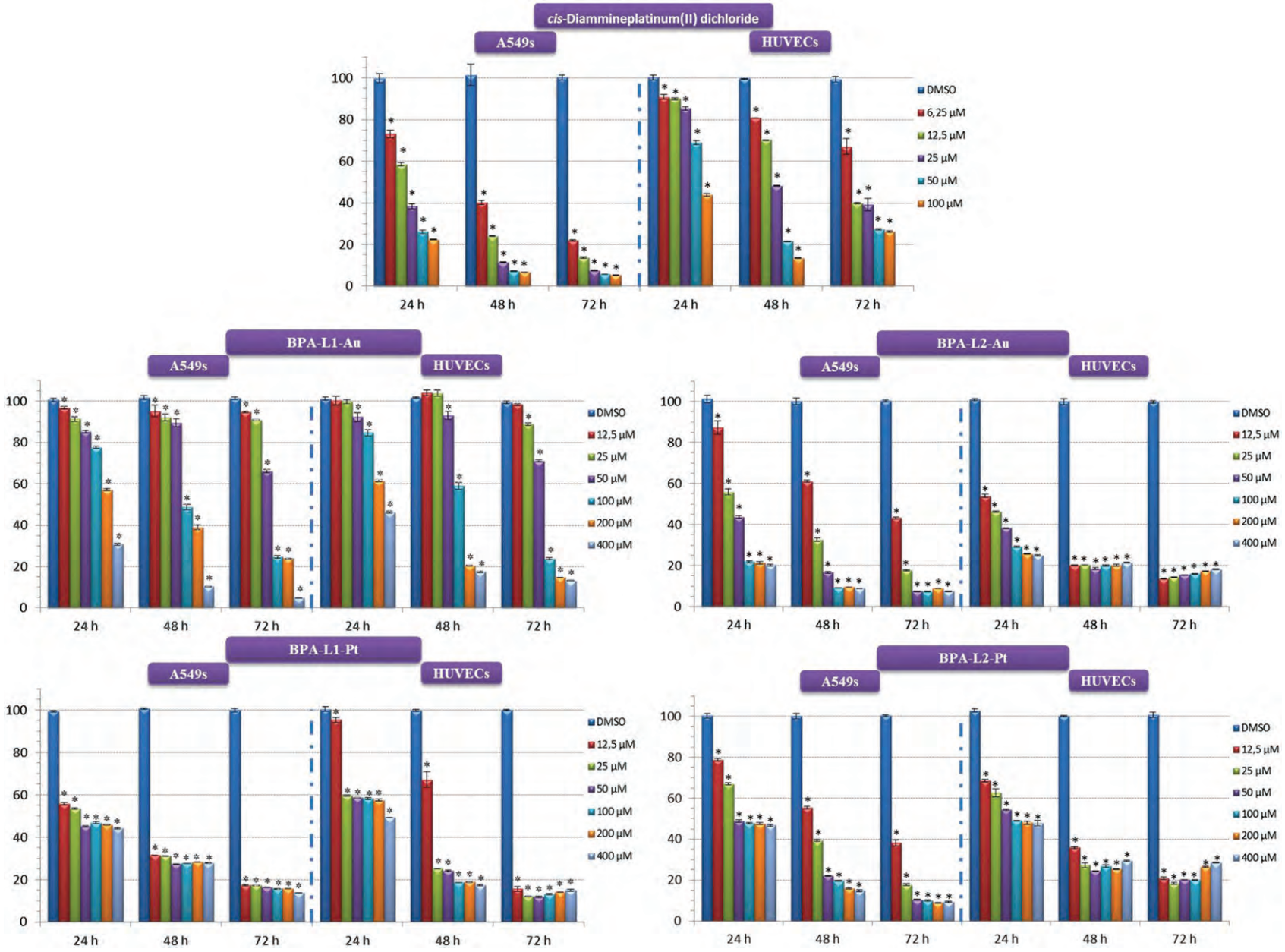

Figure 2. Anti-proliferative influences of cis-diammineplatinum (II) dichloride and the synthesized *BPA*-based complexes on human lung adenocarcinoma (A549) cells and umbilical vein endothelial cells (HUVECs).

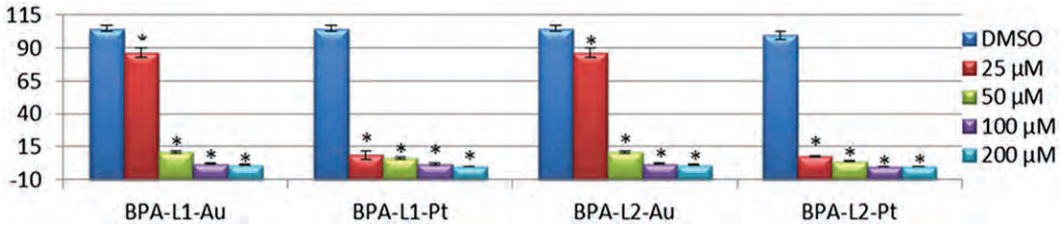

Figure 3. Percentage soft agar colony forming efficacy of A549 lung adenocarcinoma cells treated with the synthesized organometallic complexes for 15 days.

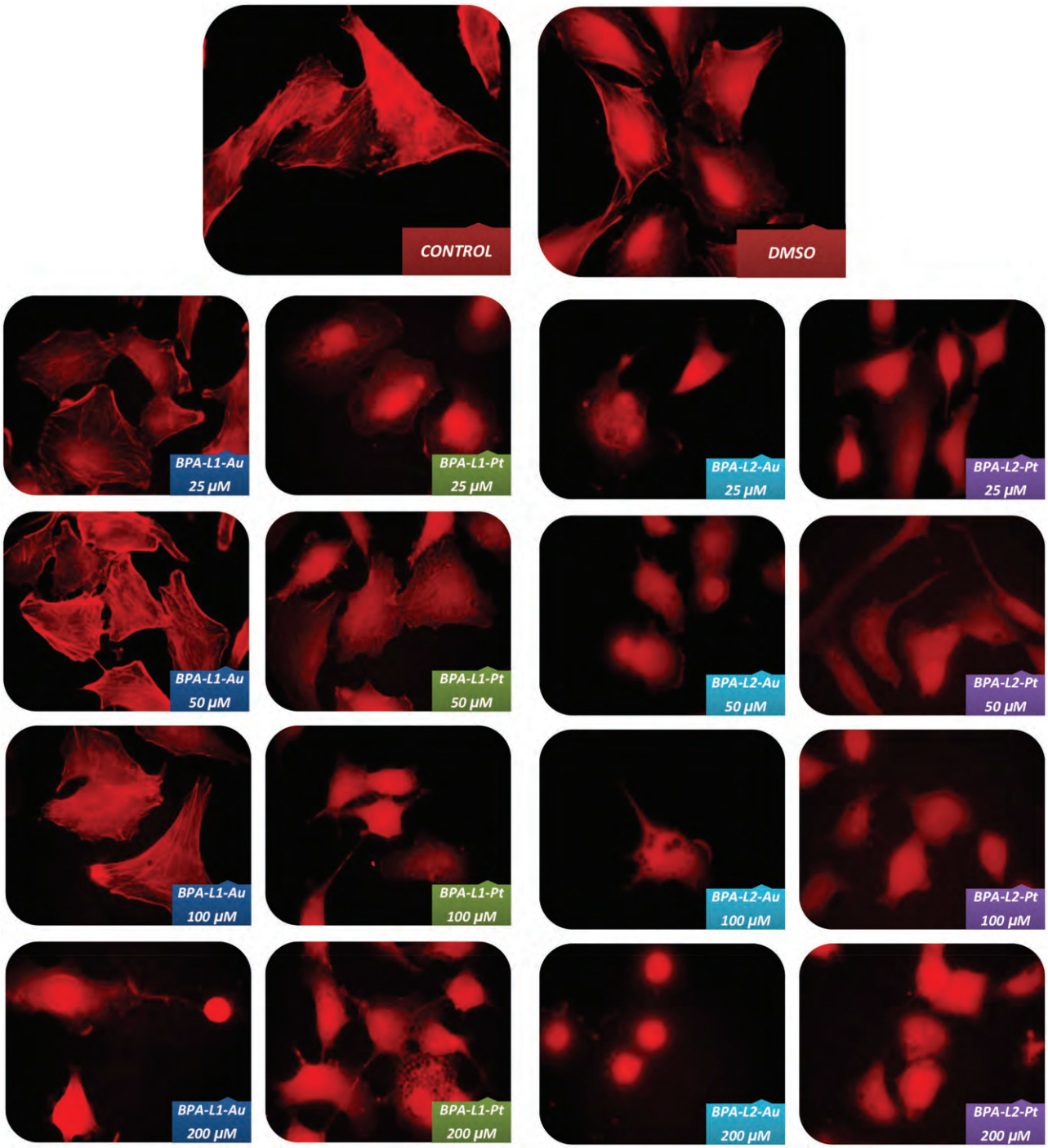

Figure 4. The alterative influence of the synthesized organometallic complexes on filamentous actin cytoskeleton proteins in the A549 cancer cell line.

of the synthesized *BPA*-based complexes were expected to be higher in cancer cells than noncancer cells due to the high metabolic rates and the proliferation frequencies of cancer cells. Although the *BPA-L1-Au* and *BPA-L1-Pt* complexes, which are *BPA*-based complexes from the ligand 4,4′-dimethyl-2,2′-dipyridyl (*L1*), displayed a selective cytotoxicity

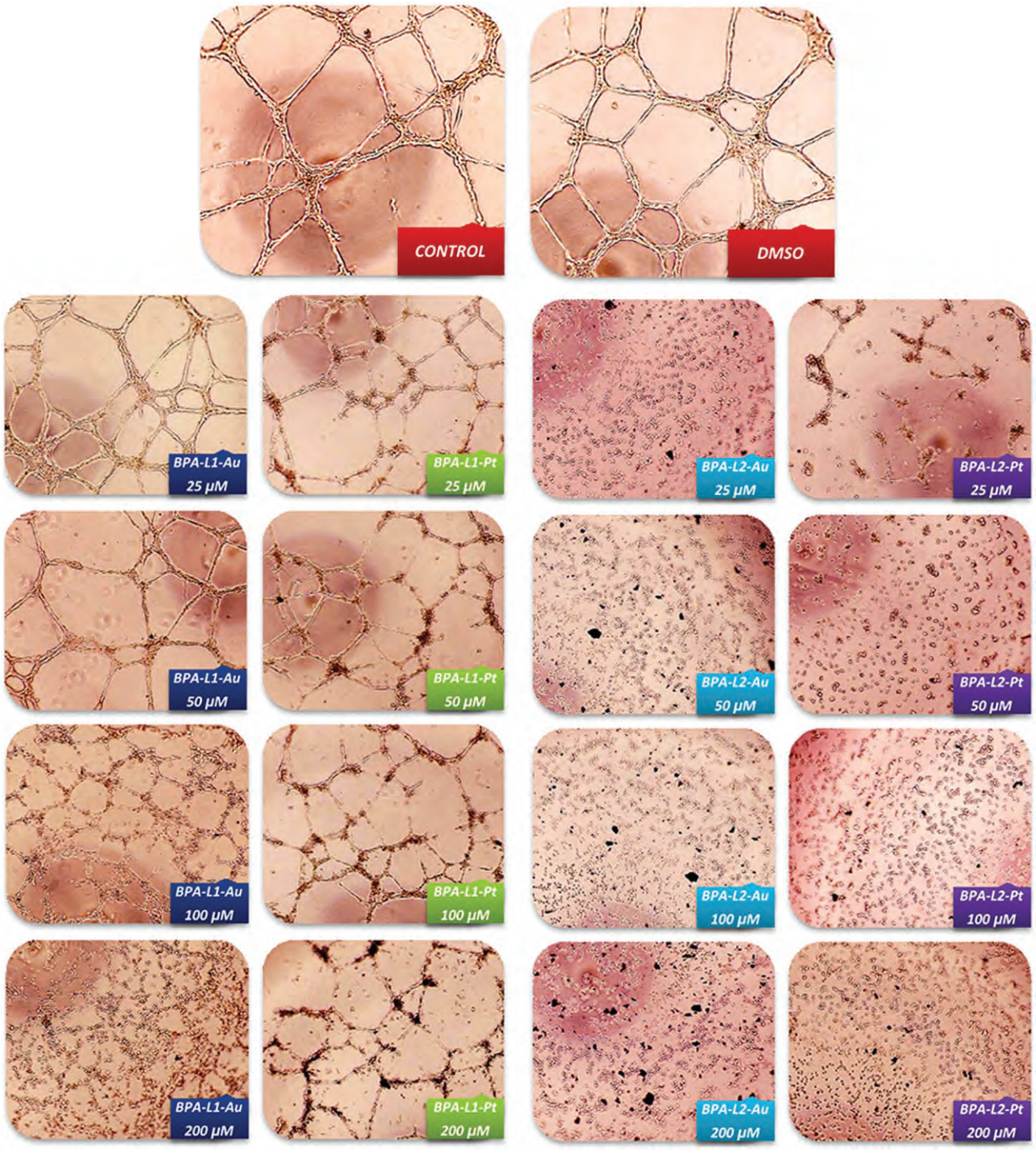

Figure 5. Activities of the synthesized organometallic complexes on human umbilical vein endothelial cell (HUVEC) tube formation and migration.

on adenocarcinoma cells, the complexes including 1,10-phenanthroline-5,6-dion (*L2*) showed opposite activities.

Consequently, boosting or reducing the cancer cell selectivity of *BPA*-based complexes is dependent on the metal and ligand type. *BPA-L1-Pt* complex, for example, was identified as the most selective cytotoxic compound for cancer cells. It showed selective anticancer activity on A549 lung adenocarcinoma cells by enhancing the activity of platinum and ligand *L1*. In contrast, the ligand *L2* acted as an obstacle for the utilization of L-amino-acid transport and the selective feature of *BPA*. Thus, new *BPA*-based organometallic complexes (ruthenium, titanium, gallium, etc.) should be designed and synthesized to boost the selectivity of *BPA* and obtain more potent drug candidates. In addition, further *in vitro* and *in vivo* activity studies should be performed using the promising complexes *BPA-L1-Pt* and *BPA-L1-Au* to understand the underlying activity mechanisms.

Acknowledgments

The authors thank Anadolu University, Bezmialem Vakif University, and Mugla Sitki Kocman University.

Disclosure statement

No potential conflict of interest was reported by the authors.

Funding

This study was supported by Anadolu University (Project no: 1101S019 – AÜBAP) and TUBITAK (Project no: 110S077 – SBAG-HD-560).

ORCID

Mehmet Varol http://orcid.org/0000-0003-2565-453X

References

Aihara, T., *et al.* 2006. First clinical case of boron neutron capture therapy for head and neck malignancies using 18F-BPA PET. *Head & Neck*, 28 (9), 850–855.

Aisen, P., Enns, C. and Wessling-Resnick, M. 2001. Chemistry and biology of eukaryotic iron metabolism. *The International Journal of Biochemistry & Cell Biology*, 33 (10), 940–959.

Alderden, R.A., Hall, M.D. and Hambley, T.W. 2006. The discovery and development of cisplatin. *Journal of Chemical Education*, 83 (5), 728.

Ali, I., *et al.* 2013. Platinum compounds: a hope for future cancer chemotherapy. *Anti-Cancer Agents in Medicinal Chemistry (Formerly Current Medicinal Chemistry-Anti-Cancer Agents)*, 13 (2), 296–306.

Andreini, C., *et al.* 2008. Metal ions in biological catalysis: from enzyme databases to general principles. *JBIC Journal of Biological Inorganic Chemistry*, 13 (8), 1205–1218.

Bost, F., *et al.* 1999. The Jun kinase 2 isoform is preferentially required for epidermal growth factor-induced transformation of human A549 lung carcinoma cells. *Molecular and Cellular Biology*, 19 (3), 1938–1949.

Bostancioglu, R.B., *et al.* 2012. Studies on the cytotoxic, apoptotic and antitumoral effects of Au (III) and Pt (II) complexes of 1, 10-phenanthroline on V79 379A and A549 cell lines. *Journal of Enzyme Inhibition and Medicinal Chemistry*, 27 (3), 458–466.

Carmeliet, P. and Jain, R.K. 2000. Angiogenesis in cancer and other diseases. *Nature*, 407 (6801), 249–257.

Chen, D., *et al.* 2009. Metal complexes, their cellular targets and potential for cancer therapy. *Current Pharmaceutical Design*, 15 (7), 777–791.

Condeelis, J., Singer, R.H., and Segall, J.E. 2005. The great escape: when cancer cells hijack the genes for chemotaxis and motility. *Annual Review of Cell and Developmental Biology*, 21, 695–718.

Corte-Real, L., *et al.* 2014. Anticancer activity of structurally related ruthenium(II) cyclopentadienyl complexes. *Journal of Biological Inorganic Chemistry*, 19 (6), 853–867.

Çağır, A., *et al.* 2017. Evaluation of multifunctional hybrid analogs for stilbenes, chalcones and flavanones. *Anti-cancer Agents in Medicinal Chemistry*, 17 (14), 1915–1923.

Dart, A. 2016. Cell migration: caged for protection. *Nature Reviews Cancer*, 17 (1), 2.

Frezza, M., Schmitt, S., and Ping Dou, Q. 2011. Targeting the ubiquitin-proteasome pathway: an emerging concept in cancer therapy. *Current Topics in Medicinal Chemistry*, 11 (23), 2888–2905.

Gao, E., *et al.* 2011. Synthesis, characterization, interaction with DNA, and cytotoxic effect in vitro of new mono-and dinuclear Pd (II) and Pt (II) complexes with benzo [d] thiazol-2-amine as the primary ligand. *Inorganic Chemistry*, 50 (11), 4732–4741.

Hanahan, D. and Weinberg, R.A. 2011. Hallmarks of cancer: the next generation. *Cell*, 144 (5), 646–674.

Heber, E.M., *et al.* 2006. Homogeneous boron targeting of heterogeneous tumors for boron neutron capture therapy (BNCT): chemical analyses in the hamster cheek pouch oral cancer model. *Archives of Oral Biology*, 51 (10), 922–929.

Henriksson, R., *et al.* 2008. Boron neutron capture therapy (BNCT) for glioblastoma multiforme: a phase II study evaluating a prolonged high-dose of boronophenylalanine (BPA). *Radiotherapy and Oncology*, 88 (2), 183–191.

Keibler, M.A., *et al.* 2016. Metabolic requirements for cancer cell proliferation. *Cancer & Metabolism*, 4 (1), 16.

Komeda, S. and Casini, A. 2012. Next-generation anticancer metallodrugs. *Current Topics in Medicinal Chemistry*, 12 (3), 219–235.

Kreja, L. and Seidel, H.-J. 2002. On the cytotoxicity of some microbial volatile organic compounds as studied in the human lung cell line A549. *Chemosphere*, 49 (1), 105–110.

Liu, W. and Gust, R. 2013. Metal N-heterocyclic carbene complexes as potential antitumor metallodrugs. *Chemical Society Reviews*, 42 (2), 755–773.

Miyatake, S.-I., *et al.* 2016. Boron neutron capture therapy for malignant brain tumors. *Neurologia Medico-Chirurgica*, 56 (7), 361–371.

Mjos, K.D. and Orvig, C. 2014. Metallodrugs in medicinal inorganic chemistry. *Chemical Reviews*, 114 (8), 4540–4563.

Mosmann, T. 1983. Rapid colorimetric assay for cellular growth and survival: application to proliferation and cytotoxicity assays. *Journal of Immunological Methods*, 65 (1), 55–63.

Nobili, S., *et al.* 2010. Gold compounds as anticancer agents: chemistry, cellular pharmacology, and preclinical studies. *Medicinal Research Reviews*, 30 (3), 550–580.

Ouchi, N., *et al.* 2004. Adiponectin stimulates angiogenesis by promoting cross-talk between AMP-activated protein kinase and Akt signaling in endothelial cells. *Journal of Biological Chemistry*, 279 (2), 1304–1309.

Ronconi, L., *et al.* 2006. Gold (III) dithiocarbamate derivatives for the treatment of cancer: solution chemistry, DNA binding, and hemolytic properties. *Journal of Medicinal Chemistry*, 49 (5), 1648–1657.

Rosselli, S., *et al.* 2012. Cytotoxic effect of eudesmanolides isolated from flowers of *Tanacetum vulgare* ssp. siculum. *Molecules*, 17 (7), 8186–8195.

Rubin, L., *et al.* 1991. A cell culture model of the blood-brain barrier. *The Journal of Cell Biology*, 115 (6), 1725–1735.

Sahai, E. 2005. Mechanisms of cancer cell invasion. *Current Opinion in Genetics & Development*, 15 (1), 87–96.

Serratrice, M., *et al.* 2012. Synthesis, structural characterization, solution behavior, and in vitro antiproliferative properties of a series of gold complexes with 2-(2′-pyridyl) benzimidazole as ligand: comparisons of gold (III) versus gold (I) and mononuclear versus binuclear derivatives. *Inorganic Chemistry*, 51 (5), 3161–3171.

Sun, R.W.-Y. 2013. Strategies to improve the anti-cancer properties of gold (III) complexes. *Modern Chemistry & Applications*, 1 (102), 2.

Varol, M. 2016. The importance of metal-based drugs in medicinal inorganic chemistry to improve life quality of patients. *Journal of Applied Pharmacy*, 8 (1), 1–2.

Varol, M., *et al.* 2016. Photoprotective activity of vulpinic and gyrophoric acids toward ultraviolet B-induced damage in human keratinocytes. *Phytotherapy Research*, 30 (1), 9–15.

Wang, Y., *et al.* 2015. Metallomic and metalloproteomic strategies in elucidating the molecular mechanisms of metallodrugs. *Dalton Transactions*, 44 (2), 437–447.

Wheate, N.J., *et al.* 2010. The status of platinum anticancer drugs in the clinic and in clinical trials. *Dalton Transactions*, 39 (35), 8113–8127.

Yamaguchi, H., Wyckoff, J., and Condeelis, J. 2005. Cell migration in tumors. *Current Opinion in Cell Biology*, 17 (5), 559–564.

Yokoyama, K., *et al.* 2006. Pharmacokinetic study of BSH and BPA in simultaneous use for BNCT. *Journal of Neuro-oncology*, 78 (3), 227–232.

Zhao, Y., Butler, E.B., and Tan, M. 2013. Targeting cellular metabolism to improve cancer therapeutics. *Cell Death & Disease*, 4 (3), e532.